Semiconductor Physics, Quantum Electronics & Optoelectronics, 2025. V. 28, No 3. P. 315-321.

Hetero- and low-dimensional structures

Bilayer MoS_2 phototransistor deposited on a flexible substrate

S.G. Petrosyan[1,*], A.M. Khachatryan[1], P.G. Petrosyan[2]

[1]*Institute of Radiophysics and Electronics, NAS of Armenia, Ashtarak, 0204, Armenia*
[2]*Institute of Physics, Yerevan State University, Yerevan, 0025, Armenia*
[*]*Corresponding author e-mail: stepan.petrosyan@rau.am*

Abstract. A new phototransistor with a MoS_2 bilayer deposited on a polyimide substrate was fabricated using pulsed-laser deposition technique. The structural and optical properties of the bilayer MoS_2 films were characterized by Raman, photoluminescence and optical absorption spectroscopy. The photocurrent generated by a laser light with the wavelength of 532 nm in the top gate flexible field effect transistor was determined for specified drain and gate voltages. The photoresponsivity of the device could be adjusted over a wide range by controlling the gate and drain voltages. At this, the photoresponsivity value could exceed 12.5 mA/W. The structure showed switching behavior with a characteristic time of approximately 10 ms in response to pulsed illumination. The photocurrent changed significantly due to compressive or tensile strain induced by the bent substrate, which affected the band-gap value of the ultrathin MoS_2 layers. The proposed structure may find potential applications in flexible electronics, such as *e.g.* for nanoscale flexible photodetectors or stress sensors.

Keywords: bilayer MoS_2, flexible substrate, phototransistor, strain.

https://doi.org/10.15407/spqeo28.03.315
PACS 85.60.Dw

Manuscript received 09.04.25; revised version received 04.08.25; accepted for publication 03.09.25; published online 24.09.25.

1. Introduction

Recently, a great interest has been drawn to 2D semiconducting materials such as MoS_2. This transition-metal dichalcogenade exhibits interesting electrical, optical and mechanical properties that correlate with its layered structure [1].

Using band and strain engineering, various functional 2D heterostructures for applications in high-performance optoelectronics, such as *e.g.* for photodetectors covering a wide spectral range from infrared to ultraviolet one [2–6] can be designed.

It is well known that a layered MoS_2 crystal consists of triple-layered sheets with hexagonally distributed Mo atoms in the middle, which have strong covalent bonding to six sulfur atoms in the top and bottom layers. At this, the inter-sheet stacking is maintained by the van der Waals forces [1]. Such weak interaction between the neighboring sheets having no surface dangling bonds enables growing MoS_2 on various substrates without need to account for possible lattice mismatch. Such substrates may include organic polymers, in particular polyimide (PI). Direct growth of 2D materials on flexible substrates is a big step toward fabrication of 2D flexible devices [7–9].

Numerous fabrication approaches, including sputtering, chemical vapor deposition and molecular beam epitaxy, have been used to grow 2D materials. Unfortunately, most of the synthesis processes, in particular, the widely exploited chemical vapor deposition, use the growth temperatures above 500 °C and therefore are not compatible with polymers that have low thermal stability [10, 11].

In contrast, the temperature during pulsed laser deposition (PLD) is relatively low, enabling direct growth of 2D materials on different plastic substrates. The PLD also offers other advantages for preparing various layered 2D materials and structures on a large scale [12–14]. It can be used to transfer the target material to different substrates according to their stoichiometric ratio. In this method, the layer imperfection and the band gap of the 2D material can be efficiently controlled by simply manipulating the energy and number of laser pulses.

It is well established that optical properties of 2D layered semiconductors are highly controlled by the number of the layers owing to the quantum confinement effects in the out-of-plane direction and changes in symmetry [15, 16]. Despite their high (more than 97% [17]) optical transparency, mono- or few-layer 2D materials can strongly interact with incident light, which leads to enhanced photon absorption. This absorption stems from existence of the Van Hove singularities in the electronic density of states and formation of strongly-bound excitons/trions induced by the reduced thicknesses [18–20].

Moreover, atomic thickness of 2D layered materials provides extraordinary mechanical flexibility. Flexible bending of substrates can cause mechanical strain in ultrathin layers, which changes the inter-atomic distances. Such changes can impact material properties such as band gap value, optical absorption coefficient and carrier mobility [4, 9, 19, 21]. Note that the strain effects may be significant for 2D materials without any bending. For example, the thermal expansion coefficient of 2D MoS_2 highly exceeds that of plastic or rigid substrates [22], which causes a tension in the thin film during post-growth cooling.

It has been demonstrated that atomically thin MoS_2 is a promising channel material for field-effect phototransistors (FET) with a high current ON/OFF ratio, a low sub-threshold slope, and high photoresponsivity in the wide spectral range [23].

Hence, direct synthesis of high-quality MoS_2 on plastic substrates is of high demand for flexible and wearable optoelectronic devices.

The main objectives of this study are to fabricate phototransistors based on bilayer (2L) MoS_2 on PI substrates using the PLD method and to make a detailed analysis of their dark and light-induced electric properties.

2. Experimental results and discussions

2.1. Preparation of 2L MoS_2 phototransistor

A Q-switched Nd laser was used to deposit thin films consisting of a few atomic monolayers of MoS_2. The laser operated at a wavelength of 1.064 μm, pulse duration of 30 ns, pulse energy of 0.35 J, pulse repetition rate of 0.1 Hz, and beam diameter of 20 mm. A 50 μm thick polyimide film was chosen as a flexible substrate due to its exceptional physical, electrical and mechanical properties, which remain stable over a wide temperature range (up to 400 °C).

Ultrathin MoS_2 layers were grown by DC magnetron sputtering using a target in form of a pressed tablet of MoS_2 and sulfur powders taken in such weight ratio that the atomic ratio of Mo:S in the target was 1:4 [13]. For the growth process, the target and the substrate were located in the growth chamber at a distance of 3 to 6 cm from each other. The vacuum level in the chamber was maintained no worse than 10^{-5} mm Hg. The substrate was heated to 200 °C.

After the growth, the films were annealed at 200 °C for 5 min and then cooled down to room temperature. The thickness of the MoS_2 films can be controlled by the number of pulses used to grow the films. Typically, 5 laser pulses are sufficient to grow one monolayer of MoS_2 under the used technological conditions [13]. The grown films had good adhesion to the polyimide substrate.

Prior to fabricating a MoS_2 phototransistor, we characterized the deposited 2L MoS_2 films by measuring their photoluminescence (PL), optical transmittance and Raman spectra.

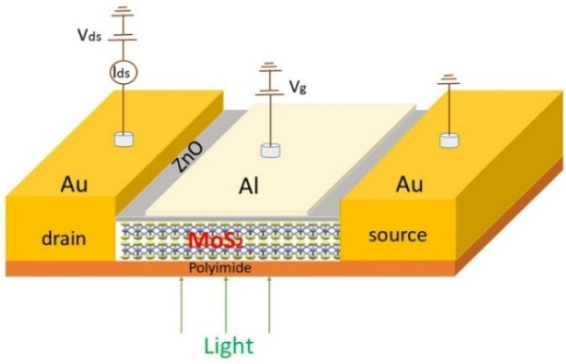

Fig. 1. Schematic view of a 2L MoS_2 FET structure with electrical contacts. The direction of incident light used to characterize the device is indicated.

We fabricated a FET using 2L MoS_2 as the conductive channel and a 100 nm thick transparent *i*-ZnO (high-k dielectric) layer as the top-gate dielectric. This allows for low power consumption due to an increased gate capacitance and enhanced mobility caused by the dielectric screening effect [24]. 100 nm thick gold layers deposited on the PI substrate prior to the 2L MoS_2 film deposition were used as the source and drain. An Al gate electrode was deposited onto the gate dielectric (see Fig. 1). The gate length and width were 5 nm and 1 mm, respectively. The electrical transport properties of the 2L MoS_2 FET were measured in the dark and under illumination of a green laser with $\lambda = 532$ nm at powers of up to 70 μW at room temperature.

2.2. Structure characterization

During a standard experiment, an ultrathin MoS_2 layer was directly deposited onto a polyimide substrate along with gold drain and source electrodes. The film thickness controlled by the number of ablating laser pulses was approximately 1.2 nm. The film consisted of two monolayers as was identified by Raman spectroscopy investigations.

The PL spectra of the deposited films were measured at room temperature using an excitation laser with a wavelength of 532 nm. It can be seen from Fig. 2a that the PL spectrum shows two clear emission peaks A and B at 1.89 and 2.01 eV, respectively. These peaks are related to direct radiative recombination of photo-generated electron-hole pairs that form two types of excitons corresponding to the spin-orbital split valleys of the valence band at the K-point of the Brillouin zone [25, 26]. The peak energy separation (approximately 0.11 eV) corresponds to spin-orbital splitting of the valence band at the K-point of the Brillouin zone. An apparently dominant peak A points to a low density of non-radiative recombination defects and high sample quality [26]. The asymmetric shape of the emission peak A may be caused by trion contribution, which can be more prominent in 2L MoS_2 as compared to 1L MoS_2 [20, 22].

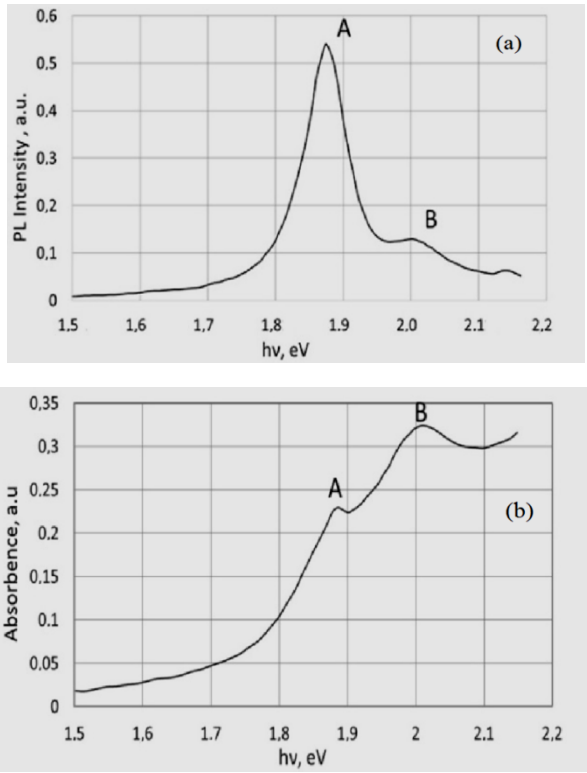

Fig. 2. PL (a) and optical absorbance (b) spectrum of 2L MoS_2 grown on PI substrate by PLD (A – 1.88 eV, B – 2.02 eV).

Optical absorbance of the 2L MoS_2 as a function of photon energy is presented in Fig. 2b. It can be seen from this figure that the film is characterized by high absorbance in the visible range. In particular, absorbance for the photon energies greater than 1.8 eV exceeds 10%. The absorption peaks A and B at 1.89 and 2.01 eV in Fig. 2b match the PL resonances in both position and width. Therefore, they may be attributed to direct excitonic transitions between the spin-orbital split valence band maxima and conduction band minimum, all located at the K-point of the Brillouin zone. The absorption (emission) tail in the photon energy range of 1.5 to 1.8 eV is due to indirect transitions between the valence band maximum and the conduction band minimum at the Γ-point of the Brillouin zone [15, 25, 26].

Since Raman spectroscopy is a powerful tool for determining vibrational modes of atomically thin 2D materials, we used it to further describe the deposited MoS_2 films and verify their thickness and properties (Fig. 3). Two typical Raman active modes of hexagonal MoS_2 at 385 and 407 cm^{-1} were observed, which can be attributed to in-plane E^1_{2g} and out-of-plane A_{1g} lattice vibrations, respectively [27]. Separation between the E^1_{2g} and A_{1g} peaks depends on the number of MoS_2 single layers, which makes it possible to determine the number of the layer in the synthesized samples from the Raman spectra [27, 28]. Using an empirical relation for the variation of this interpeak separation with the number of the monolayers in MoS_2 thin films [13, 27], this value is found to be about 22.6 cm^{-1} for the bilayer MoS_2.

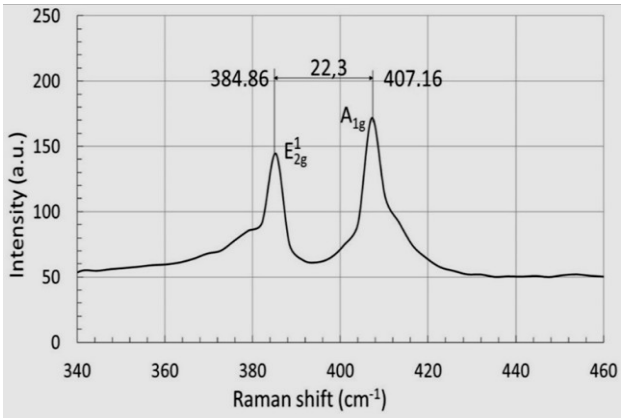

Fig. 3. Raman spectrum of 1.2 nm thick MoS_2 film grown on PI substrate by PLD.

This value is very close to the measured value of 22.3 cm^{-1} shown in Fig. 3. The narrowness of the main Raman peak A_{1g} (FWHM = 4 cm^{-1}) is indicative of the high crystalline quality of the synthesized film. The small difference between these values may be attributed to the possible effect of the strain caused by the mismatch between the thermal expansion coefficients of the PI substrate and deposited MoS_2 layer [21, 29].

The MoS_2-based phototransistor was investigated by studying its output characteristics, such as generated photocurrent and photoresponsivity, as well as its switching behavior at different values of optical power, and gate and drain voltage.

The effect of the mechanical strain exerted on the bent flexible substrate was also studied. The gating (transfer) characteristics of our FET are shown in Fig. 4 confirming that it is a typical FET with an *n*-type channel. Varying the gate voltage V_g from negative to low positive values does not significantly affect the characteristics, thus indicating that the top gate is unlikely to accumulate trapped charges during the experiment.

2.3. Photocurrent (PC)

As the device was illuminated by a green laser with the wavelength λ = 532 nm at room temperature, the drain current increased by several orders of magnitude. The output curves in the dark and under illumination are shown in Fig. 5. It can be seen from this figure that our transistor exhibits current saturation at high drain voltages V_{ds}. The saturation current under the "pinch-off" conditions increases with the illumination power and also depends on the back gate voltage.

The device photoresponsivity (R_{ph}) defined as I_{ph}/P_{light} (here, I_{ph} is the difference between the PC and the dark current and P_{light} is the total optical power, respectively) depends on the drain and gate voltages. For example, at $V_g = 0$ V and $V_{ds} = 4.5$ V, R_{ph} is approximately equal to 5 mA/W (Fig. 6). When the gate voltage increases to 40 V, R_{ph} becomes higher than 12.5 mA/W, thus proving that the top gate plays an important role in controlling photocurrent in the 2L MoS_2 phototransistor.

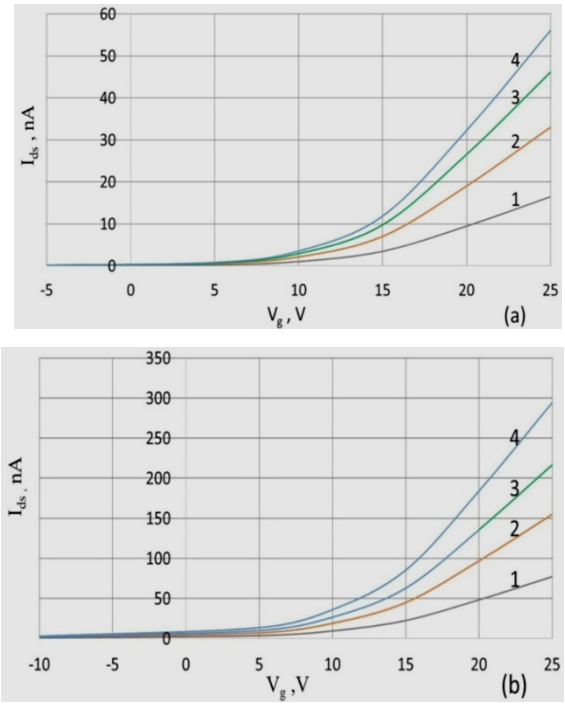

Fig. 4. Gating response (transfer characteristics) of MoS_2 phototransistor in the dark (a) and under illumination at a power of 10 μW (b), acquired at the top gate voltage V_g varying from –10 to +25 V and at different drain voltages V_{ds} = 1 V (*1*), 2 (*2*), 3 (*3*), and 4 (*4*).

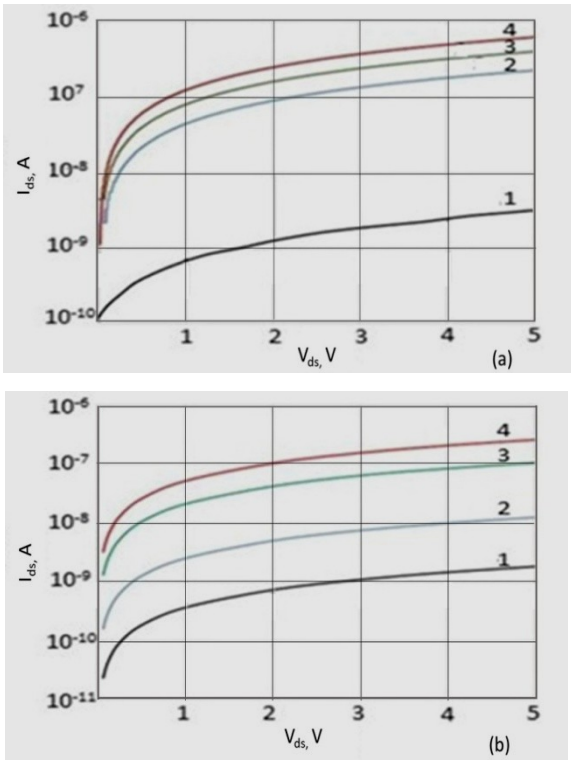

Fig. 5. (a) Output (I_{ds}–V_{ds}) characteristics of the device at V_g = 0 V in the dark and under illumination at different power values: in the dark (*1*), 0.5 (*2*), 1 (*3*), and 5 μW (*4*). (b) (I_{ds}–V_{ds}) characteristics under illumination (5 μW) at different gate voltages V_g = 0 (*1*), 10 (*2*), 20 (*3*), and 30 V (*4*).

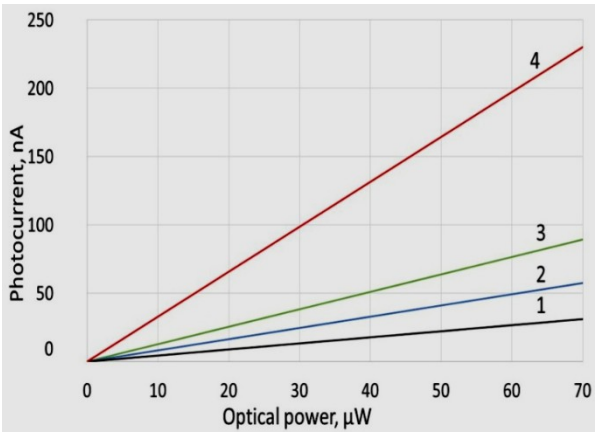

Fig. 6. PC of FET as a function of illumination power measured at V_g = 0 V and different drain voltages V_{ds} = 0.5 (*1*), 1 (*2*), 1.5 (*3*), and 4 V (*4*). The device is illuminated from the PI substrate side.

As shown in Fig. 6, the PC measured at V_g = 0 V and at different drain voltages is proportional to the illumination power due to an increase in the electron-hole pair generation rate caused by light absorption in the MoS_2 layer.

A sharp rise/decay of the PC was observed when the radiation was either turned ON or OFF for all the drain and gate voltages (Fig. 7). The response time (defined as the time to reach 90% of the maximum PC after switching the light from OFF to ON) and the recovery time (defined as the time to reach 10% of the maximum PC after switching light from ON to OFF) were estimated to be 12 and 25 ms, respectively. Such an abrupt rise and decay of the PC observed for different values of the drain (gate) voltage and illuminating light power can be explained by the lack of metastable charge carrier trapping centers in the bulk of the MoS_2 and at the interfaces.

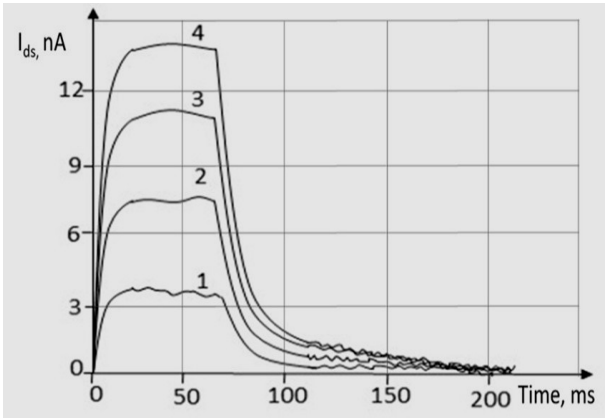

Fig. 7. Dynamical photo-switching behavior of phototransistor at V_g = 0 V and V_{ds} = 4 V for different illumination power P_{light} (μW): 10 (*1*), 20 (*2*), 30 (*3*), and 40 (*4*). The laser is turned on for 75 ms and then turned off.

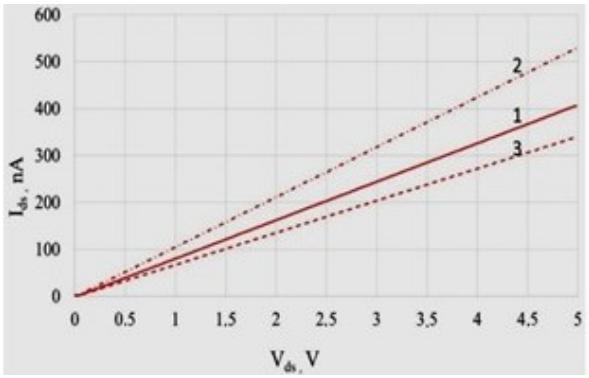

Fig. 8. PC as a function of V_{ds} before the substrate bending (*1*) and after its convexly (*2*) or concavely (*3*) curving ($\varepsilon = \pm 0.5\%$). The curving of the substrate induces a tensile (*2*) or compressive stress (*3*) in the film, respectively. The gate voltage $V_g = 0$ V and the illumination power is 1 μW.

To evaluate the influence of bending on the MoS_2-based phototransistor, PC as a function of the drain voltage was measured before and after the bending. In general, as shown in Fig. 8a, the PC can significantly change even when a slight stress is applied. In the experiment, the flexible MoS_2 FET was placed in bending molds with convex or concave curvatures. The uniaxial strain applied to the sample, estimated as the ratio of the substrate thickness (h_{PI}) to twice the radius (R) of curvature ($\varepsilon \approx h_{PI}/2R$), was 0.5% for h_{PI} = 50 μm and R = 5 mm. The mechanical stress σ_{bend} in the MoS_2 film related to the bending strain can be estimated using the following expression [30]:

$$\sigma_{bend} = \frac{E_{PI} h_{PI}^2}{6 d_{\mathrm{MoS2}} R (1 - \nu_{PI})}, \quad (1)$$

where E_{PI} and ν_{PI} are the Young modulus and the Poisson ratio of the substrate, respectively, and d_{MoS2} is the MoS_2 film thickness. The value of E_{PI} used in the calculations was 2.5 GPa for polyimide films (as indicated by the manufacturer [31]) and ν_{PI} was fixed at 0.34. The estimated value of σ_{bend} was 263 GPa.

In general, the total stress in a 2L MoS_2 is composed of the stress induced by bending and the thermal stress originating from a mismatch in the coefficients of thermal expansion (CTE) between the PI substrate and the thin MoS_2 film. Polyimide films are characterized by the CTE value $\alpha_{PI} = 11 \cdot 10^{-6}$ 1/C [31], which is usually much larger than that of 2L MoS_2 ($\alpha_{\mathrm{MoS2}} = 0.5 \cdot 10^{-6}$ 1/C [29]). Therefore, during cooling down from the elevated temperature corresponding to the deposition process (approximately 200 °C) to room temperature, the PI film shrinks at a high rate, which results in a biaxial compressive stress in the MoS_2. In other words, the MoS_2 films grown on the PI substrates were always under a certain compressive stress even without any bending. The thermal stress (σ_{th}) can be expressed as follows [32]:

$$\sigma_{th} = E_{\mathrm{MoS2}} (E_{PI} - E_{\mathrm{MoS2}}) (T_{dep} - T_{measure}), \quad (2)$$

where E_{MoS2}, α_{MoS2}, α_{PI}, T_{dep}, and $T_{measure}$ are the Young modulus of MoS_2, CTEs of MoS_2 and the polyimide film, and the sample temperatures during the deposition and the measurement, respectively. It is noteworthy that the Poisson effect is neglected in Eq. (2). The temperatures T_{dep} and $T_{measure}$ were set to 200 °C and 25 °C, respectively, and E_{MoS2} for 2L MoS_2 was set to 270 GPa [21, 33]. The value of σ_{th} estimated by Eq. (2) is 0.74 GPa, which is a negligible value compared to the bending induced stress.

We may conclude therefore that when the PI film is convexly curved upward, the MoS_2 film deposited on its upper surface is subjected to a tensile stress. Conversely, when the MoS_2 film is deposited on the concave side of a bent PI substrate, it is subjected to a compressive stress. Convex bending, as is known, results in a reduction of the band-gap of 2L MoS_2 due to the tensile strain [21], while concave bending leads to an increase in the band gap of the MoS_2 [34, 35]. A decrease in the band gap led to the increased light absorption by the MoS_2. As a result, for a given laser intensity, and the drain and gate voltage, the structure exhibited a larger photoresponse compared to the case of a flat substrate. Under the same conditions, concave bending (compressive strain), increasing the band gap, should lead to a decreased light absorption and, therefore, lower device photocurrent as shown in Fig. 8.

3. Conclusions

In summary, employing the low-temperature PLD method, we fabricated a 2L MoS_2-based flexible phototransistor and conducted a detailed investigation of its electric and photoelectric characteristics. Under fixed drain and gate voltages, the PC is depended only on the illumination intensity. The photoresponsivity of the device can be adjusted over a wide range by controlling the gate and drain voltages and can be higher than 12.5 mA/W. This parameter for the flexible 2L MoS_2 phototransistor fabricated on a polyimide substrate is not inferior to that of a phototransistor based on graphene or 1L MoS_2 [2, 3, 5].

We have shown that generation and recombination of non-equilibrium carriers in our device can be switched within tens of ms. Such prompt photo-switching behavior controlled by incident light highlights the stability of the device characteristics.

We observed a pronounced change in the PC due to bending-induced strain variation in the band gap. This observation confirms the viability of strain engineering as a powerful tool for creating new flexible and tunable photodetectors based on several-layer MoS_2 deposited on PI substrates. Among the potential applications of such few-layer MoS_2 structures there are nanoscale stress sensors and displays.

Declaration of competing interest

The authors declare no competing financial interests or personal relationships to the reported paper.

Data availability

The reported data can be available from the corresponding authors upon request.

References

1. N. Briggs N., Subramanian Sh., Lin Zh. *et al.* A roadmap for electronic grade 2D materials. *2D Mater.* 2019. **6**. P. 022001. https://doi.org/10.1088/2053-1583/aaf836.
2. Nalwa H.S. A review of molybdenum disulfide (MoS_2) based photodetectors: from ultra-broadband, self-powered to flexible devices. *RSC Adv*. 2020. **10**. P. 30529–30602. https://doi.org/10.1039/d0ra03183f.
3. Choi W., Cho M.Y., Konar A. *et al.* High-detectivity multilayer MoS_2 phototransistors with spectral response from ultraviolet to infrared. *Adv. Mater.* 2012. **24**. P. 5832–5836. https://doi.org/10.1002/adma.201201909.
4. Yan Y., Ding Sh.,Wu X. *et al*. Tuning the physical properties of ultrathin transition-metal dichalcogenides *via* strain engineering. *RSC Adv*. 2020. **10**. P. 39455–39467. https://doi.org/10.1039/D0RA07288E.
5. Xie Ch., Mak Ch., Tao X. *et al*. Photodetectors based on two-dimensional layered materials beyond graphene. *Adv. Funct. Mater.* 2017. **27**. P. 1603886–1-41. https://doi.org/10.1002/adfm.201603886.
6. Esposito F., Bosi M., Attolini G., Golovynskyi S. *et al*. Two-dimensional MoS_2 for photonic applications. *SPQEO*. 2025. **28**. P. 37–46. https://doi.org/10.15407/spqeo28.01.037.
7. Singh E., Singh P., Kim K.S. *et al.* Flexible molybdenum disulfide atomic layers for wearable electronics and optoelectronics. *ACS Appl. Mater. Interfaces.* 2019. **11**. P. 11061–11105. https://doi.org/10.1021/acsami.8b19859.
8. Ma Zh., Zhang Y., Zhang K. *et al.* Recent progress in flexible capacitive sensors: structures and properties. *Nano Mater. Sci*. 2023. **5.** P. 265–277. https://doi.org/10.1016/j.nanoms.2021.11.002.
9. Sahatiya P., Madhava Ch., Shinde A. *et al.* Flexible substrate based few layer MoS_2 electrode for passive electronic devices and interactive frequency modulation based on human motion. *IEEE Trans. Nanotechnol*. 2018. **17**. P. 338–344. https://doi.org/10.1109/TNANO.2018.2802649.
10. Gong Y., Li B., Ye G. *et al*. Direct growth of MoS_2 single crystals on polyimide substrates. *2D Mater.* 2017. **4**. P. 021028–1-6. https://doi.org/10.1088/2053-1583/aa6fd2.
11. Van der Zande A.M., Huang P.Y., Chenet D.A. *et al*. Grains and grain boundaries in highly-crystalline monolayer molybdenum disulfide. *Nat. Mater.* 2013. **12**. P. 554–561. https://doi.org/10.1038/nmat3633.
12. Wang B., Zhang Z.B. *et al.* Recent progress in high performance photo-detectors enabled by the pulsed laser deposition technology. *J. Mater. Chem. C*. 2020. **8**. P. 4988–5014. https://doi.org/10.1039/c9tc07098b.
13. Petrosyan S., Khachatryan A. Atomically thin layers of MoS_2 grown by the method of pulsed laser deposition. *J. Contemp. Phys.* 2021. **56**. P. 234–239. http://doi.org/10.3103/S1068337221030191.
14. Kumar S., Sharma A., Ho Y.T. *et al.* High performance UV photo-detector based on MoS_2 layers grown by pulsed laser deposition technique. *J. Alloys Compd*. 2020. **835**. P. 55222. https://doi.org/10.1016/j.jallcom.2020.155222.
15. Mak K.F., Lee Ch., Hone J. *et al.* Atomically thin MoS_2: A new direct-gap semiconductor. *Phys. Rev. Lett*. 2010. **105**. P. 136805–1-4. https://doi.org/10.1103/PhysRevLett.105.136805.
16. Jin W., Yeh P-Ch., Zaki N. *et al*. Direct measurement of the thickness-dependent electronic band structure of MoS_2 using angle-resolved photoemission spectroscopy. *Phys. Rev. Lett*. 2013. **111**. P. 106801. https://doi.org/10.1103/PhysRevLett.111.106801.
17. Buscema M., Island J.O., Groenendijk D.J. *et al.* Photocurrent generation with two-dimensional van der Waals semiconductor. *Chem. Soc. Rev.* 2015. **44**. P. 3691–3718. https://doi.org/10.1039/c5cs00106d.
18. Klots A.R., Newaz A.K.M., Wang B. *et al.* Probing excitonic states in suspended two-dimensional semiconductors by photocurrent spectroscopy. *Sci. Rep*. 2014. **4**. P. 6608. https://doi.org/10.1038/srep06608.
19. Yang L., Cui X., Zhang J. *et al.* Lattice strain effects on the optical properties of MoS_2 nanosheets. *Sci. Rep.* 2015. **4**. P. 5649–1-7. https://doi.org/10.1038/srep05649.
20. Golovynskyi S., Datchenko O.I., Dong D. *et al*. Trion binding energy variation on photoluminescence excitation energy and power during direct to indirect bandgap crossover in monolayer and few-layer MoS_2. *J. Phys. Chem. C.* 2021. **125.** P. 17806–17819. https/doi.org/10.1021/acs.jpcc.1c04334.
21. Conley H.J., B. Wang B., Ziegler J.I. *et al.* Bandgap engineering of strained monolayer and bilayer MoS_2. *Nano Lett.* 2013. **13**. P. 3626–3630. https://doi.org/10.1021/nl4014748.
22. Golovynskyi S., Datsenko O.I., Perez-Jimenez A.I. *et al*. Exciton and trion at the perimeter and grain boundary of CVD-grown monolayer MoS_2 strain effect influencing application in nano-optoelectronics. *ACS Appl. Nano Mater.* 2024. **7**. P. 15570–15582. https://doi.org/10.1021/acsanm.4c02284.
23. Lee H.S., Baik S.S., Lee K. *et al.* Metal semiconductor field-effect transistor with MoS_2/conducting NiO_x van der Waals Schottky interface for intrinsic high mobility and photoswitching speed. *ACS Nano*. 2015. **9**. P. 8312–8320. https://doi.org/10.1021/acsnano.5b02785.
24. Yu Zh., Ong Zh.-Y., Pan Y. *et al.* Realization of room temperature phonon limited carrier transport in monolayer MoS_2 by dielectric and carrier screening. *Adv. Mater.* 2016. **28**. P. 547–552. https://doi.org/10.1002/adma.201503033.
25. Cheiwchanchamnangij T., Lambrecht W.R.L. Quasiparticle band structure calculation of monolayer, bilayer and bulk MoS_2. *Phys. Rev. B*. 2012. **85**. P. 205302. https://doi.org/10.1103/PhysRevB.85.205302.
26. McCreary K.M., Hanbicki A.T., Sivaram S.V. *et al.* A- and B-exciton photoluminescence intensity ratio as a measure of sample quality for transition metal dichalcogenide monolayers. *APL Mater.* 2018. **6**. P. 111106. https://doi.org/10.1063/1.5053699.

27. Li H., Zhang Q., Yap C.C.R. *et al*. From bulk to monolayer MoS_2: evolution of Raman scattering. *Adv. Funct. Mater.* 2021. **22.** P. 1385–1390. https://doi.org/10.1002/adfm.201102111.
28. Zhang X., Han W.P., Wu J.B. *et al.* Raman spectroscopy of shear and layer breathing modes in multilayer MoS_2. *Phys. Rev. B*. 2013. **87**. P. 115413–1-8. https://doi.org/10.1103/PhysRevB.87.115413.
29. Lin Zh. *et al.* Thermal expansion coefficient of few-layer MoS_2 studied by temperature-dependent Raman spectroscopy. *Sci. Rep.* 2021. **11**. P. 7037–1-9. https://doi.org/10.1038/s41598-021-86479-6.
30. Kamikawa Y., Masuda T., Nishinaga J. *et al.* Influence of argon pressure on sputter-deposited molybdenum back contacts for flexible $Cu(InGa)Se_2$ solar cells on polyimide films. *Solar Energy*. 2022. **241.** P. 327–334. https://doi.org/10.1016/j.solener.2022.06.006.
31. DuPont Kapton: Summary of properties, available at: https://www.dupont.com.
32. Thornton J.A., Hoffman D.W. Stress-related effects in thin films. *Thin Solid Films*. 1989. **171**. P. 5–31. https://doi.org/10.1016/0040-6090(89)90030-8.
33. Al-Quraishi K.K. *et al.* Mechanical testing of two-dimensional materials: a brief review. *Int. J. Smart Nano Mater*. 2020. **11**. P. 207–246. https://doi.org/10.1080/19475411.2020.1791276.
34. Zhang W., Zhao Z., Yang Y. *et al.* Paraffin-enabled compressive folding of two-dimensional materials with controllable broadening of the electronic band gap. *ACS Appl. Mater. Interfaces.* 2021. **13**. P. 40922–40931. https://doi.org/10.1021/acsami.1c11269.
35. Kumar A., Xu L., Pal A. *et al*. Strain engineering in 2D FETs: Physics, status, and prospects. *J. Appl. Phys.* 2024. **136**. P. 090901. https://doi.org/10.1063/5.0211555.

Authors' contributions

Petrosyan S.G.: conceptualization, supervision, investigation, writing – original draft, writing – review & editing.
Khachatryan A.M.: investigation, data curation.
Petrosyan P.G.: investigation, formal analysis, writing – original draft.

All the authors discussed the results and approved the final version of the manuscript.

Authors and CV

Stepan Petrosyan, Head of Semiconductor Nanoelectronics Laboratory of the Institute of Radiophysics and Electronics NAS RA. In 2011 he was elected a Corresponding Member of the Armenian National Academy of Sciences. He authored over 140 publications, 6 patents, and 5 monographs and textbooks. The areas of his research include thin-film solar cells, nanowire and quantum solar cells, contact phenomena in low-dimensional electron systems, quantum well, wire and dot devices, IR photodetectors, and 2D materials and devices.
https://orcid.org/ 0000-0003-1746-7005

Ashot Khachatryan, Research Fellow at the Institute of Radiophysics and Electronics of the National Academy of Sciences of Armenia. He is the author of more than 30 publications, 1 patent, and 2 monographs. The areas of his research include technology of thin-film solar cells, thin films, IR photo-detectors, and 2D materials and devices.
E-mail: khachatryanashot@yahoo.com,
https://orcid.org/0000-0002-5981-555X

Petik Petrosyan, Associate Professor at the Institute of Physics of the Yerevan State University (Armenia). He is the author over 40 publications and 4 patents. The area of his scientific interests includes semiconductor and ceramic technology, nano materials, semiconductor devices, and 2D materials.
E-mail: ppetros@ysu.am,
https://orcid.org/ 0009-0008-4190-7692

Фототранзистор на основі двошарового MoS_2, нанесений на гнучку підкладку

S.G. Petrosyan, A.M. Khachatryan, P.G. Petrosyan

Анотація. Новий фототранзистор на основі двошарового MoS_2, нанесеного на поліімідну підкладку, виготовлено методом імпульсного лазерного осадження. Структурні та оптичні властивості двошарових плівок MoS_2 охарактеризовано, використовуючи раманівську спектроскопію, фотолюмінесценцію та спектроскопію оптичного поглинання. Фотострум, що генерується лазерним світлом з довжиною хвилі 532 нм у гнучкому польовому транзисторі з верхнім затвором, визначено для заданих напруг стоку та затвора. Фоточутливість пристрою можна регулювати в широкому діапазоні, задаючи значення напруги затвора та стоку, і вона може перевищувати 12,5 мА/Вт. Під дією імпульсного освітлення структура проявляє властивість перемикання з характерним часом близько 10 мс. Фотострум значно змінюється через деформацію стискання або розтягу, викликану вигнутістю підкладки, що впливає на ширину забороненої зони в ультратонких шарах MoS_2. Запропонована структура може знайти потенційне застосування для створення гнучких електронних приладів, таких як нанорозмірний гнучкий фотодетектор або датчик напруги.

Ключові слова: двошаровий MoS_2, гнучка підкладка, фототранзистор, деформація.